Polarization Model Representation of Hydrogen Fluoride for Use in Gas- and Condensed-Phase Studies

FRANK H. STILLINGER

Bell Laboratories, Murray Hill, New Jersey 07974, U.S.A.

Abstract

The polarization model, originally developed to describe deformable and ionizable water molecules, has been extended to hydrogen fluoride. Since electronic polarization is explicitly included, the interaction energy in aggregates of molecules (with or without ions) is nonadditive. The model properly describes the structure of $(HF)_2$, including off-axis bending of the proton acceptor molecule. Calculations are presented to illustrate elementary gas-phase reactions involving proton transfer between HF and F^-, and H_2F^+ and F^-.

1. Introduction

Recently a "polarization model" was devised to describe the molecular behavior of water in both gas and condensed phases [1]. Beside accounting for the interactions operative between intact molecules, this polarization model includes the possibility of molecular vibration, ionic dissociation, and electrostatically induced polarization. The primary goal in proposing the model was to bridge the gap between spectroscopy and molecular quantum mechanics on the one hand, and the conceptual and computational demands of statistical mechanics and kinetic theory on the other hand.

While the results derived from the first polarization model study of water are certainly encouraging, it is not obvious that the same general approach could be made to work for other substances. It is the objective here to show that hydrogen fluoride can similarly be treated.

Section 2 reviews the basic strategy underlying construction of polarization models. The procedure for selecting specific functions in the model to describe hydrogen fluoride appears in Sec. 3, as do results implied for dimerization. Section 4 displays some results concerning elementary proton-transfer processes. Finally, Sec. 5 presents some ideas on directions for future evolution of the polarization model concept, including new materials applications and key data that could best be supplied by accurate computational quantum mechanics.

Formal theory necessary to develop dynamics and statistical mechanics for polarization models will appear elsewhere [2].

It must be stressed that exhaustive studies have *not* been carried out to optimize the polarization model for HF and its ionic fragments. Instead the present work is a feasibility study to show qualitative merit for the general procedure. The fact that all calculations reported here were carried out on a desk calculator indicates one important advantage that this approach seems to offer; namely, its simplicity compared to computational quantum mechanics.

2. Polarization Model

The primary objective of the model is to provide a practical means of estimating Φ, the ground-state potential-energy surface, for arbitrary nuclear configuration. In this context each nucleus is regarded as a dynamically distinct entity. Chemical bonding of these nuclei into molecular aggregates arises strictly from the behavior of Φ, and will only be a permanent feature if initial dynamical conditions so decree. We shall adhere to the convention that Φ vanishes when all distances are infinite.

Each atomic species i is assigned an invariant electrostatic charge q_i; i.e., the chemical oxidation state for each element is specified at the outset. As was the case in the preceding water study, hydrogen will be assigned charge $+e$ to correspond to a bare hydrogen nucleus. Fluorine then will be regarded as the anionic species F^-, with charge $-e$.

Species i will also be assigned scalar polarizability α_i, as an attribute of its complement of electrons. Inclusion of this electronic polarizability is mandatory in order to yield a realistic account of dielectric behavior. Hydrogen constitutes a degenerate case; since it involves a nucleus devoid of electrons in the oxidation state chosen, its polarizability vanishes.

It is convenient to split Φ into two parts:

$$\Phi = \Phi_I + \Phi_{II} \tag{1}$$

The first comprises pair interactions for each pair of nuclei in the system:

$$\Phi_I = \sum_{i<j=1}^{N} \phi_{ij}(r_{ij}) \tag{2}$$

while the second, Φ_{II}, provides a many-body interaction (not resolvable into pair terms) whose functional structure is patterned after the polarization interaction of conventional electrostatics. If Φ_I alone were present, the resulting formalism would conform to the family of "central force models" that has been investigated previously for associated liquids [3–7].

Φ_{II} is determined by the charges q_i and by the moments μ_j that they induce. We first write:

$$\mu_j = \alpha_j \mathbf{G}_j \tag{3}$$

where the linear vector field $\mathbf{G}_j$ at nucleus j arises from charges and moments of the other nuclei:

$$\mathbf{G}_j = -\sum_{l(\neq j)} \frac{\mathbf{r}_{jl} q_l}{r_{jl}^3}[1 - K_j(r_{jl})] - \sum_{m(\neq j)} \frac{\mathbf{T}_{jm} \cdot \mu_m}{r_{jm}^3}[1 - K_j(r_{jm})]$$
$$\mathbf{T}_{jm} = 1 - 3\mathbf{r}_{jm}\mathbf{r}_{jm}/r_{jm}^2 \tag{4}$$

The factors $1 - K_j$ account for spatial extension of the polarizable electron distribution surrounding nucleus j; in their absence Eq. (4) would yield the local

electric field at j. Then Φ_{II} is obtained in the following form:

$$\Phi_{II} = \frac{1}{2} \sum_{\substack{j,l \\ (j \neq l)}} \frac{(\boldsymbol{\mu}_j \cdot \mathbf{r}_{jl})q_l}{r_{jl}^3}[1 - L_j(r_{jl})] \tag{5}$$

The factors $1 - L_j$ are also introduced to account for spatial extension of the electron distribution. With the exception of nonpolarizable hydrogen (H^+), one pair of functions K_j, L_j must be determined for each chemically distinct species present.

In order to find the vector $\boldsymbol{\mu}_j$ needed in evaluation of polarization energy Φ_{II}, it is necessary to solve the coupled linear equations (3) and (4). Thus far all experience with the polarization model indicates that the requisite solution to these equations can be constructed by simple (and rapidly converging) iteration.

One can show on general grounds that the factors $1 - K_j$ and $1 - L_j$ must vanish at least cubically as $r \to 0$.

3. Function Selection

Four functions must be determined to describe pure hydrogen fluoride: ϕ_{FF}, ϕ_{FH}, K_F, L_F. Only the last three appear in the expression for the diatomic potential of the single hydrogen fluoride molecule

$$\Phi(r) = \phi_{FH}(r) - (\alpha_F e^2/2r^4)[1 - K_F(r)][1 - L_F(r)] \tag{6}$$

The corresponding dipole moment function in easily found to be

$$\mu(r) = er - (\alpha_F e/r^2)[1 - K_F(r)] \tag{7}$$

Spectroscopic properties of the single molecule can be used to provide constraints on ϕ_{FH}, K_F, and L_F. Properties of hydrogen-bonded complexes containing more than one fluoride must be invoked to provide corresponding information for ϕ_{FF}.

We have used the following value for the fluoride polarizability:

$$\alpha_F = 0.8207 \text{ Å}^3 \tag{8}$$

which is intended to represent the mean electronic polarizability of the HF molecule. This value was obtained by polynomial interpolation among polarizabilities for neon (0.3900 Å^3) [8], oxygen in water (1.4440 Å^3) [9], and nitrogen in ammonia (2.2600 Å^3) [10].

Single-molecule properties that have been accepted as relevant input from experiment are these:

(1) $r_e = 0.9170$ Å, the equilibrium bond length [11].

(2) $\mu = 1.82 \times 10^{-18}$ esu cm, the dipole moment of the molecule at r_e [12].

(3) $d\mu/dr = 1.50 \times 10^{-10}$ esu, the dipole derivative evaluated at r_e [13].

(4) $d^2\Phi/dr^2 = 1389.4$ kcal/mol Å^2, the curvature of the diatomic potential function at its minimum [5].

(5) $\Phi(r_e) = -374.446$ kcal/mol, the binding energy of $H^+ + F^-$ in formation of HF.

Needless to say, these data do not uniquely determine the required functions. But we have used them to select a set of analytic functions with globally acceptable shapes to represent ϕ_{FH}, K_F, and L_F for use in studies with the general polarization model method. The specific choices are shown in the Appendix. They yield HF molecules obeying conditions 1–5.

With respect to ϕ_{FF}, we have endeavored to have the method produce acceptable binding energies and fluoride–fluoride distances in the bifluoride anion [14], and in the HF dimer [15]. The Appendix exhibits our final choice.

When graphed each of the four functions appears qualitatively similar to its counterpart in the polarization model for water [1].

The minimum energy structure for the bifluoride anion FHF⁻ implied by the polarization model is linear, with a symmetrical hydrogen bridge. The distance between fluorines in this structure is 2.278 Å, which agrees closely (by construction) with crystallographically observed distances of about 2.27 Å [16]. The polarization model binding energy relative to separated HF and F⁻ fragments is 57.531 kcal/mol; this magnitude was accepted to yield consistency with Waddington's thermodynamic calculation [17] of the formation enthalpy of FHF⁻.

Optimized structures for two versions of the HF dimer are shown in Figure 1. The first [Fig. 1(a)] involves monomers "frozen" at their equilibrium bond lengths $r_e = 0.917$ Å. The second [Fig. 1(b)] is entirely unconstrained and thus required a full configuration space search. Upon relaxing the frozen monomers the dimer binding increases from 5.473 to 6.160 kcal/mol.

These results for FHF⁻ and (HF)₂ show that the polarization model passes an important test, namely, that it has the capacity to describe linear hydrogen bonds in hydrogen fluoride aggregates. In addition the off-axis bending of the proton-acceptor molecule in the dimer is automatically produced, in qualitative agreement both with gas-phase dimer studies [15] and with the zigzag chains of hydrogen bonds found in crystalline HF [18].

4. Proton-Transfer Processes

One of the simplest proton-transfer processes involving HF is the attachment of H⁺ to the neutral molecule to form the fluoronium cation H_2F^+. We find that the polarization model predicts this species to be a nonlinear triatomic, with symmetry C_{2v}. The F—H bonds have lengths 1.005 Å, and form an angle of 103.6° at the fluorine. The energy required to dissociate H_2F^+ into HF and H⁺ is found to be 133.962 kcal/mol. These compare moderately well with *ab initio* Hartree–Fock calculations by Diercksen *et al.* [19] who found the bond length to be 0.95 Å, the angle to be 114.75°, and the dissociation energy to be 120.1 kcal/mol. No doubt improved agreement could be obtained with a slightly modified set of polarization model functions.

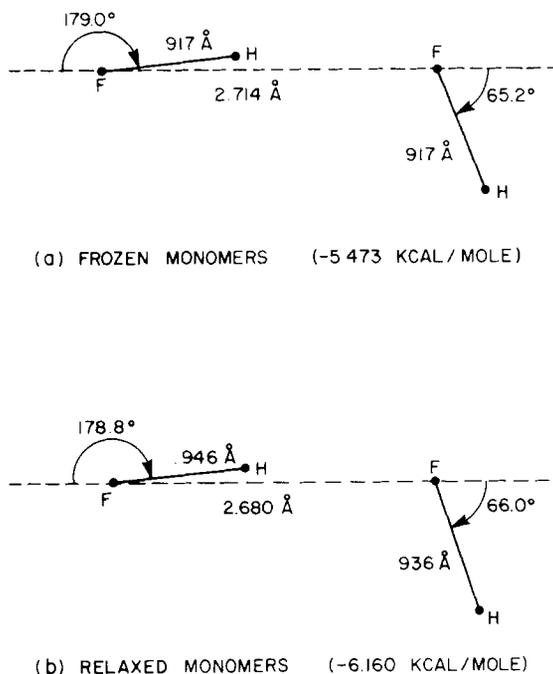The bifluoride anion mentioned in Sec. 3 can be regarded as the halfway point in a proton transfer between F⁻ and HF:

$$F^- + HF \rightleftharpoons FH + F^- \tag{9}$$

179.0°

917 Å

H

F

2.714 Å

F

65.2°

917 Å

H

(a) FROZEN MONOMERS   (-5.473 KCAL/MOLE)

178.8°

.946 Å

H

F

2.680 Å

F

66.0°

936 Å

H

(b) RELAXED MONOMERS   (-6.160 KCAL/MOLE)

Figure 1. Optimal $(HF)_2$ dimer structures for the polarization model. (a) Participating monomers are constrained to have their equilibrium bond length 0.917 Å. (b) They are permitted to relax to the global minimum without constraint. Both structures are planar.

In order to illustrate the reaction surface for this exchange process predicted by the polarization model we have performed a series of constrained-minimum energy optimizations. The results are shown in Figure 2.

The two curves appearing in Figure 2 represent energies for linear configurations of the three particles. One, containing the absolute minimum, refers to the symmetrical arrangement with H^+ midway between the two F^- particles. The other involves placing the H^+ asymmetrically between the F^- particles in such a way that the energy (at fixed F—F separation) is minimized.

Beyond the critical distance 2.428 Å the lowest energy is achieved with H^+ asymmetrically placed nearer one fluorine or the other. In this regime the approaching reactants F^- and HF retain identity. As the separation decreases toward the critical value, the HF bond length increases. The rate of change of this increase diverges as the critical distance is approached from above. The critical separation 2.428 Å thus represents a geometric catastrophe at which the H^+ reaches the midpoint, and at which F^- and HF reactants lose distinguishability. Elementary considerations suffice to show that the asymmetrical structure curve in Figure 2 terminates in a 3/2-power branch point at the catastrophe. By contrast the symmetrical structure curve is analytic there.
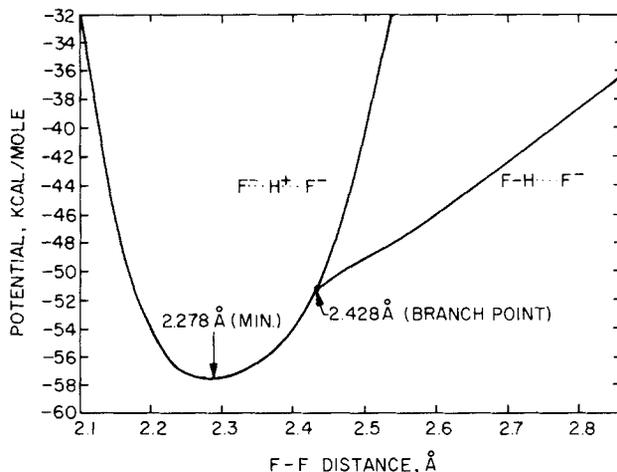
Figure 2. Energy of linear FHF⁻ according to the polarization model. Energy origin corresponds to widely separated fragments F⁻ and HF. Curve for the symmetrical structure includes the global minimum. Curve for optimized asymmetrical structure terminates in a branch point.

It hardly needs to be mentioned that the dynamical course of collision between F⁻ and HF in the gas phase will not precisely track the potential-energy curves shown in Figure 2. Instead rotational and vibrational motions will cause upward excursions from those curves at each F—F separation. The precise orbits generated by a given set of initial conditions require integration of the specific polarization model equations of motion [2]. Nevertheless, the partial characterization of the reaction offered by the constrained-potential curves in Figure 2 is useful, if not vivid.

A slightly more complex proton-transfer process is the following gas-phase neutralization reaction:

$$F^- + H_2F^+ \rightarrow HF + HF \tag{10}$$

This reaction is strongly exothermic; the polarization model places reactants 240.484 kcal/mol higher in energy than products (all unexcited).

Figure 3 presents constrained-minimum curves for reaction (10). These curves show local energy minima in the subspaces of constant F—F separation, plotted as functions of that separation. The upper curve corresponds to distinguishable reactants, the lower curve to products. The reactant curve terminates at separation 2.57 Å, once again manifesting 3/2-power branch point behavior. The geometric catastrophe that this reflects is again sudden stretch of an H—F bond.

Although previous remarks about rotational and vibrational excitation again apply, Figure 3 still gives a simple guide to the dynamical course of the neutralization reaction (10). Reactants accelerate toward each other, down the upper curve in Figure 3, under the influence of their mutual Coulomb attraction. They
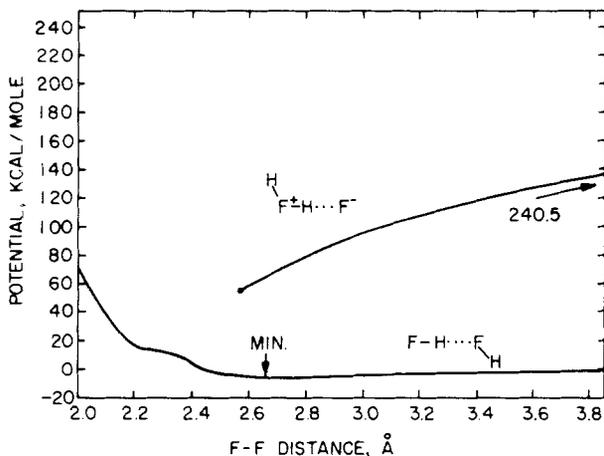
Figure 3. Constrained-minimum energy curves for neutralization reaction (10). Upper (reactant) curve ends at a branch point symptomatic of sudden proton transfer.

pass the branch point on their way inward to the highly excited region of small F—F separation. Eventually they exit from this reaction-complex region either as highly excited product molecules, or alternatively back up the reactant curve to unreacted (but possibly fluorine-exchanged) ions.

The polarization model could similarly be useful in study of more general neutralization reactions between cluster ions:

$$(HF)_m F^- + (HF)_n H^+ \to \text{products} \qquad (11)$$

where the "products" may involve two or more neutral clusters. Curves similar to those displayed in Figure 3 could be calculated as a function of the separation between centroids of fluoride sets for the respective clusters. Branch point catastrophes would locate positions at which neutralization by proton transfer could first occur without the necessity of surmounting an intervening potential energy barrier.

5. Discussion

Since the polarization model offers a feasible and efficient procedure for describing pure H_2O and pure HF separately, the way is open for consideration of their mixtures. As bulk liquids these media can contain moderately high concentrations of solvated protons. In the context of molecular dynamics computer simulation one would thereby have a way to study details of proton solvation, transport, and chemical reactivity in aqueous systems.

In modeling H_2O–HF mixtures the only new requirement would be identification of the pair potential ϕ_{OF} for oxygen–fluorine interactions. Accurate quantum-mechanical calculations to give the stable geometries and binding

energies of the species $(H_2O)HF$, $(H_2O)F^-$, and $HF(H_3O)^+$ would provide valuable input for this identification. But in parallel with that effort it would be important to test the validity of simple combining rules such as the geometric mean prescription:

$$\phi_{OF}(r) = [\phi_{OO}(r)\,\phi_{FF}(r)]^{1/2} \tag{12}$$

If their reliability could be quantitatively established, such combining rules would effect enormous simplification in description of general mixtures via the polarization model scheme.

It is attractive now to consider extension of the polarization model to include NH_3. The ability of the model to reproduce the known molecular geometry and inversion barrier has in fact already been established [20]. Further progress is currently impeded by lack of accurate geometries and energies for the species $(NH_3)_2$ and $(NH_3)NH_2^-$ (with full geometry search). It is reasonable to anticipate success in modeling pure NH_3, and to its successful incorporation in polarization models of aqueous solutions to produce solvated NH_4^+ ions.

Inclusion of other monovalent ions in the general polarization model program should present no special problems. Greater challenge and interest may be generated by multivalent ions. The case of B^{3+} is particularly interesting on account of the borate glasses that form upon thermal dehydration of orthoboric acid, H_3BO_3. These glass networks have structures whose details are uncertain at present [21], but which could conceivably be illuminated by a properly exploited polarization model.

Appendix

When they are expressed in terms of Å and kcal/mol as the distance and energy units, respectively, the polarization model functions that have been determined for hydrogen fluoride are as follows:

$$\phi_{FH}(r) = (332.1669/r)\,[10\exp(-A_1 r) - 1]$$

$$-[A_2 + A_3(r - r_e) + A_4(r - r_e)^2]\exp[-18(r - r_e)^2] \tag{13}$$

$$\phi_{FF}(r) = (332.1669/r) + \exp[-7(r - 2.695)]$$

$$+\frac{15.0}{1 + \exp[3(r - 2.591)]} + \frac{31.8}{1 + \exp[18(r - 2.367)]} \tag{14}$$

$$1 - K_F(r) = r^3/\{r^3 - B_1(r - r_e)^2\exp[-9(r - r_e)] + B_2\exp(-B_3 r)\} \tag{15}$$

$$1 - L_F(r) = 1 - \exp(-C_1 r)[1 + C_1 r + \tfrac{1}{2}C_1^2 r^2 - C_2 r^3 + C_3 r^4] \tag{16}$$

These expressions utilize parameter values

$$r_e = 0.917$$

$$A_1 = 4.241\ 788\ 626, \qquad A_2 = 39.072\ 277\ 40$$

$$A_3 = 42.639\ 179\ 15, \qquad A_4 = 826.004\ 799\ 2 \tag{17}$$

$$B_1 = 3.032\ 915\ 939, \qquad B_2 = 36.723\ 787\ 85, \qquad B_3 = 4.437\ 614\ 774$$

$$C_1 = 3.489\ 640\ 131, \qquad C_2 = 16.774\ 500\ 25, \qquad C_3 = 24.390\ 403\ 85$$

Bibliography

[1] F. H. Stillinger and C. W. David, J. Chem. Phys. **69**, 1473 (1978).
[2] F. H. Stillinger, J. Chem. Phys., to be published.
[3] H. L. Lemberg and F. H. Stillinger, J. Chem. Phys. **62**, 1677 (1975).
[4] A. Rahman, F. H. Stillinger, and H. L. Lemberg, J. Chem. Phys. **63**, 5223 (1975).
[5] F. H. Stillinger, Israel J. Chem. **14**, 130 (1975).
[6] H. L. Lemberg and F. H. Stillinger, Mol. Phys. **32**, 353 (1976).
[7] F. H. Stillinger and A. Rahman, J. Chem. Phys. **68**, 666 (1978).
[8] E. U. Condon and H. Odishaw, *Handbook of Physics*, 2nd ed. (McGraw-Hill, New York, 1967), pp. 7–40.
[9] D. Eisenberg and W. Kauzmann, *The Structure and Properties of Water* (Oxford U.P., New York, 1969), p. 15.
[10] H. H. Landolt and R. Bornstein, *Zahlenwerte und Funktionen* (Springer-Verlag, Berlin, 1951), Vol. 1, pt. 3, p. 511.
[11] G. Herzberg, *Molecular Spectra and Molecular Structure. Vol. I. Spectra of Diatomic Molecules* (Van Nostrand, New York, 1950), p. 537.
[12] R. D. Nelson, Jr., D. R. Lide, Jr., and A. A. Maryott, *Selected Values of Electric Dipole Moments for Molecules in the Gas Phase*, NSRDS-NBS 10 (U.S. G.P.O., Washington, D.C., 1967).
[13] R. Lovell and W. Herget, J. Opt. Soc. Amer. **52**, 1374 (1962).
[14] L. Pauling, *The Nature of the Chemical Bond*, 3rd ed. (Cornell U.P., Ithaca, 1960), pp. 460–462.
[15] T. R. Dyke, B. J. Howard, and W. Klemperer, J. Chem. Phys. **56**, 2442 (1972).
[16] S. N. Vinogradov and R. H. Linnell, *Hydrogen Bonding* (Van Nostrand Reinhold, New York, 1971), p. 184.
[17] T. C. Waddington, Trans. Faraday Soc. **54**, 25 (1958).
[18] M. Atoji and W. N. Lipscomb, Acta Crystallogr. **7**, 173 (1954).
[19] G. H. F. Diercksen, W. von Niessen, and W. P. Kraemer, Theor. Chim. Acta (Berlin) **31**, 205 (1973).
[20] C. W. David, private communication.
[21] L. D. Pye, V. D. Frechette, and N. J. Kriedl, Eds., *Borate Glasses: Structure, Properties, Application* (Plenum, New York, 1978).